Compton profile of cuprous oxide by linear combination of Gaussian orbitals

1996 J. Phys.: Condens. Matter 8 5139

(http://iopscience.iop.org/0953-8984/8/27/022)

J. Phys.: Condens. Matter **8** (1996) 5139–5148. Printed in the UK

Compton profile of cuprous oxide by linear combination of Gaussian orbitals

Aniruddha Deb and Arun Kumar Chatterjee

Department of Physics, Bose Institute, Calcutta 700 009, India

Received 18 October 1995, in final form 7 February 1996

Abstract. In this paper we report self-consistent all-electron local-density calculations using the linear combination of Gaussian orbitals method for cuprous oxide. We calculated the directional Compton profile and their anisotropic effect. The spherical average Compton profile has also been calculated and compared with the experimental results. We also calculated the density of states of cuprous oxide.

1. Introduction

Cuprous oxide has been studied mainly for its role in high-T_c superconductors and its excitonic spectrum [1]. It is a semiconductor with a band gap of 2.17 eV and crystallizes in a simple-cubic structure in which oxygen is tetrahedrally coordinated by copper atoms, while copper is linearly coordinated by two oxygen atoms. These low coordination numbers, which are unusual for oxides and results in the case of copper in a non-vanishing electric field gradient, are not explained by the ionic model of cuprous oxide consisting of Cu^+ cations with $3d^{10}$ configuration and O^{2-} anions. Until now work done on cuprous oxide includes a self-consistent LAPW band-structure calculation by Marksteiner *et al* [2], a recent cluster calculation by Nagel [3], a tight-binding band-structure calculation by Robertson [4], a non-self-consistent APW band-structure calculation by Dahl and Switendick [5] and a renormalized free-atom model (RFA) calculation by Bandyophyay *et al* [6]. The electronic structure of cuprous oxide was investigated by photoelectron, Auger electron and bremsstrahlung isochromat spectroscopies by Ghijsen *et al* [7]. From all these studies, Nagel's consideration that an ionic model is not appropriate for cuprous oxide and that the charge transferred from O^{2-} to Cu^+ is not used to form covalent bonds aroused our interest in calculating the Compton profile which is very sensitively dependent on the valence electron population. The latter study illustrates quite clearly the sensitivity of the anisotropy of Compton profiles to the nature of bonding in solids.

There are significant differences between the results of the various calculations mentioned above. Therefore we here made the first attempt to calculate the Compton profiles using the linear combination of Gaussian orbitals (LCGO), together with some related properties such as the density of states (DOS) and charge analysis, with the emphasis on chemical bonding.

In this paper, section 2 describes the computational procedures. The Compton profile results are presented in section 3, while the DOS under normal conditions are given in section 4. The conclusions are finally given in section 5.

0953-8984/96/275139+10$19.50

2. Computational method

This section contains a brief description of our computational procedures. We have used the LCGO method [8], which has been successfully applied to various metals [9–22]. This method does not make any shape approximation to the charge densities or potentials. The exchange–correlation potential used has the von Barth–Hedin form [23] but with parameters given by Rajagopal *et al* [24]. The calculations are made on basis of the local-density approximation to the density-functional theory. The Bloch wavefunctions needed in the self-consistent calculations were expanded in a set of independent Gaussian orbitals, including in this case, for copper, 13 s functions, ten p functions, five d functions and one f function and, for oxygen, ten s functions and six p functions and are given in table 1. For copper we have employed the given basis set except that the most diffuse s-orbital exponent was deleted and an extra p-orbital and an f-orbital were added to the original table [25–27]. We expand the Coulomb and the exchange–correlation potential in a Fourier series. The Gaussian orbitals facilitate the analytic evaluation of the integrals which occur. A Ewald-type procedure has been evolved to facilitate convergence. Calculation of the Fourier coefficients of the exchange–correlation potential requires numerical integration. In this process the unit cell is divided into touching spheres and an interstitial region. Inside the sphere, $V_{xc}(\boldsymbol{r})$ is expanded into cubic harmonics and integrated by Filon's method. In order to integrate over the interstitial region, a least-squares fit is made to $V_{xc}(\boldsymbol{r})$ in this region using only an auxiliary Fourier series. The Fourier coefficients of this series will be denoted by $V_{xc}(\boldsymbol{K})$, are rapidly convergent and are able to reproduce the potential in the interstitial region to six to ten significant digits. A new Fourier series is thus defined which reproduces the same potential in the interstitial region but zero inside the muffin-tin sphere. This contribution is then added to the results of the numerical integration in the muffin-tin sphere. In this calculation the value of the lattice constant was taken to be 8.07 au [28, 29] and the Hamiltonian and the overlap matrices considered for computation are of dimensions 75×75 for copper and 32×32 for oxygen.

The calculations were carried out to self-consistency using 89 points in the irreducible wedge of the first Brillouin zone, taking advantage of the symmetry. A systematic variation in the number of points did not give any appreciable improvement in the results. Hence the final bands were generated using 89 points, and related properties were calculated with this grid.

3. Compton profile

An analysis of the Compton profile is important since it is sensitive to the state of the valence electrons of the solids. It is one of the experimental and theoretical methods which provides a critical test of the band wavefunctions; it also provides important information on some features of the Fermi surface. In addition to this, the study of the anisotropy of the Compton profile can lead to an understanding of the nature of bonding in solids. Experimental innovations with the use of energy-dispersive detectors and high-energy γ-ray sources have extended the application of this probe to heavier solids such as the transition-metal compounds. An extensive review of the earlier works on transition metals using polycrystalline samples has been given in [30, 31].

We report in this work a computation of the Compton profile and its anisotropy in cuprous oxide. We have here considered only the valence-electron contribution to the Compton profile. This is because a Hartree–Fock contribution of core electrons for cuprous oxide can be obtained from the literature [32]. Since core electrons do not differ appreciably

Table 1. Orbital exponents of the Gaussian basis set.

Copper		Oxygen	
1s	307 637.0	1s	18 045.3
2s	46 592.90	2s	2660.12
3s	10 651.10	3s	585.663
4s	3043.310	4s	160.920
5s	1010.620	5s	51.1637
6s	374.2520	6s	17.8966
7s	150.7960	7s	6.639 01
8s	64.626 80	8s	2.076 58
9s	22.138 10	9s	0.773 60
10s	9.347 460	10s	0.255 76
11s	2.608 630		
12s	0.997 212		
13s	0.140 120		
1p	2026.050	1p	49.8279
2p	484.2700	2p	11.4887
3p	157.8030	3p	3.609 24
4p	60.484 40	4p	1.320 52
5p	25.359 30	5p	0.482 09
6p	11.168 50	6p	0.165 09
7p	4.564 110		
8p	1.884 400		
9p	0.734 735		
10p	0.155 065		
1d	53.647 80		
2d	15.074 70		
3d	5.103 920		
4d	1.727 430		
5d	0.528 322		
1f	0.8		

in the solid from those in case of a free atom, a free-atom core contribution for copper and oxygen would suffice to account for the total Compton profile.

The standard expression for the Compton profile is written as

$$J_{\hat{k}}(q) = \frac{\Omega}{(2\pi)^3} \int \mathrm{d}^3 p \, \rho(\boldsymbol{p}) \delta(q - \boldsymbol{p}\hat{k}) \tag{1}$$

in which $\rho(\boldsymbol{p})$ is the momentum distribution, $\boldsymbol{k}$ is the change in momentum after a Compton scattering has occurred; $\hat{\boldsymbol{k}} = \boldsymbol{k}/|\boldsymbol{k}|$, Ω is the volume of the unit cell,

$$q = \frac{m\omega}{|\boldsymbol{k}|} - (\tfrac{1}{2})|\boldsymbol{k}| \tag{2}$$

and $\hbar\omega$ is the energy transferred to the electron after a Compton scattering event has occurred.

The momentum density requires a summation over all occupied states. At $T = 0$ K, this can be written as

$$\rho(\boldsymbol{p}) = \sum_{n,k} \theta(E_F - E_n(\boldsymbol{k}))|\psi_n(\boldsymbol{k}, \boldsymbol{p})|^2 \tag{3}$$

where E_F is the Fermi energy, $E(\boldsymbol{k})$ is the energy of a state, θ is the unit step function and $\psi_n(\boldsymbol{k}, \boldsymbol{p})$ is the momentum space Bloch function which is related to the position space Bloch function by Fourier transformation. The directional profiles were calculated using 89 points in the irreducible wedge of the first Brillouin zone. The Compton profiles $J_{\hat{\boldsymbol{k}}}(q)$ along the [100], [110] and [111] directions together with the spherically averaged profile for each value of q ranging from 0 to 7 au are given in table 2. Differences of the Compton profile with respect to directions of the momentum transfer are shown in figure 1. The most relevant information comes from the difference between two directional Compton profiles. Such a difference reveals the anisotropic features of the momentum distribution and is related to the difference in atomic interaction along two crystallographically distinct directions. In the cuprous oxide crystal the nearest neighbour of the Cu atom is the O atom and it is in the [111] direction. The Cu–Cu atoms and O–O atoms interact in the [110] and [111] directions, respectively, Here, as the nearest-neighbour Cu–O is in the [111] direction, the calculated Compton profile in this direction is expected to represent the momentum density of the valence electrons of the cuprous oxide crystal.

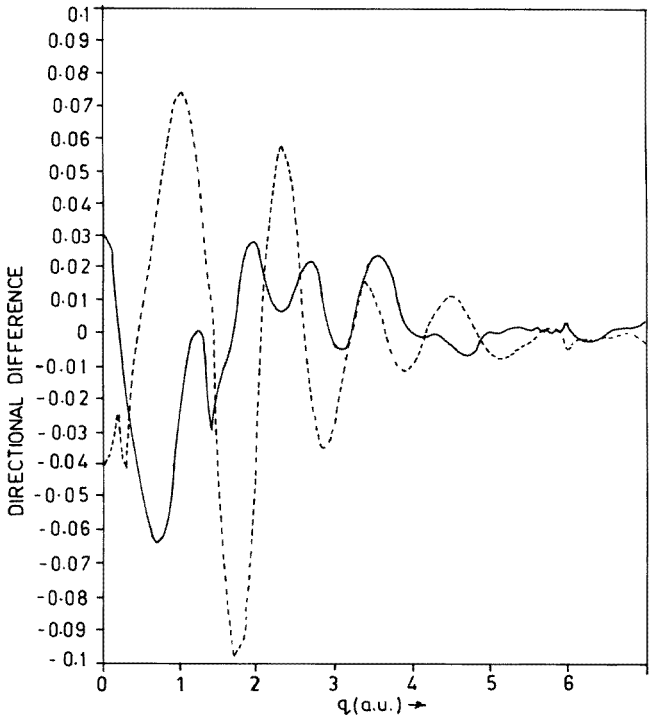

Figure 1. Theoretical anisotropy curves of Compton profiles of cuprous oxide: – – –, $J_{[110]}$–$J_{[111]}$ anisotropy; ——, the $J_{[111]}$–$J_{[100]}$ anisotropy.

A coupling between copper and oxygen is evident from the oscillatory nature of the $J[110]$–$J[111]$ anisotropies as shown in figure 1. It also predicts that there must be a strong overlap between the copper orbitals and the oxygen orbitals. In our charge analysis (table 3) it is seen that there is a charge transfer from copper to oxygen which means an overlap of orbitals, causing the oscillatory nature in the anisotropy curve $J[110]$–$J[111]$.

In the anisotropy curve $J[111]$–$J[100]$ the oscillation is small and, in the high-

Table 2. Calculated Compton profile in the [100], and [111] directions together with the directional average profile.

q (au)	$J_{[100]}$	$J_{[110]}$	$J_{[111]}$	J_{avg}
0.0	13.282	13.273	13.313	13.280
0.1	13.198	13.184	13.221	13.195
0.2	12.979	12.960	12.984	12.971
0.3	12.618	12.588	12.601	12.601
0.4	12.114	12.074	12.081	12.087
0.5	11.524	11.481	11.476	11.492
0.6	10.847	10.806	10.788	10.813
0.7	10.778	10.751	10.714	10.748
0.8	9.996	9.993	9.936	9.979
0.9	9.317	9.343	9.273	9.339
1.0	8.725	8.775	8.700	8.739
1.1	8.210	8.272	8.202	8.235
1.2	7.794	7.847	7.795	7.822
1.3	7.473	7.495	7.471	7.484
1.4	7.174	7.152	7.144	7.160
1.5	6.866	6.804	6.850	6.833
1.6	6.558	6.469	6.549	6.516
1.7	6.253	6.159	6.257	6.212
1.8	5.943	5.871	5.965	5.915
1.9	5.633	5.595	5.662	5.623
2.0	5.339	5.338	5.366	5.345
2.1	5.063	5.096	5.080	5.082
2.2	4.798	4.852	4.806	4.824
2.3	4.542	4.606	4.548	4.574
2.4	4.294	4.356	4.302	4.325
2.5	4.062	4.109	4.077	4.087
2.6	3.843	3.870	3.864	3.861
2.7	3.643	3.646	3.666	3.651
2.8	3.462	3.444	3.478	3.458
2.9	3.295	3.265	3.299	3.283
3.0	3.137	3.107	3.133	3.123
3.1	2.995	2.976	2.990	2.985
3.2	2.853	2.853	2.851	2.853
3.3	2.715	2.737	2.725	2.729
3.4	2.584	2.619	2.603	2.605
3.5	2.464	2.500	2.488	2.486
3.6	2.354	2.383	2.378	2.374
3.7	2.254	2.269	2.273	2.265
3.8	2.161	2.164	2.174	2.166
3.9	2.072	2.063	2.075	2.069
4.0	1.985	1.975	1.985	1.981
4.1	1.908	1.901	1.907	1.905
4.2	1.834	1.835	1.833	1.834
4.3	1.764	1.771	1.765	1.768
4.4	1.699	1.707	1.698	1.703
4.5	1.638	1.647	1.635	1.642
4.6	1.581	1.586	1.576	1.583
4.7	1.525	1.524	1.518	1.523
4.8	1.470	1.467	1.464	1.467
4.9	1.416	1.412	1.414	1.414
5.0	1.364	1.359	1.365	1.363
5.1	1.319	1.311	1.319	1.315

Table 2. (Continued.)

q (au)	$J_{[100]}$	$J_{[110]}$	$J_{[111]}$	J_{avg}
5.2	1.277	1.270	1.278	1.274
5.3	1.237	1.233	1.239	1.237
5.4	1.199	1.197	1.201	1.199
5.5	1.162	1.160	1.162	1.162
5.6	1.125	1.127	1.127	1.127
5.7	1.090	1.093	1.091	1.093
5.8	1.056	1.058	1.058	1.058
5.9	1.024	1.026	1.024	1.024
6.0	0.994	0.992	0.998	1.000
6.1	0.965	0.962	0.964	0.964
6.2	0.937	0.933	0.935	0.935
6.3	0.909	0.905	0.907	0.905
6.4	0.883	0.879	0.881	0.879
6.5	0.856	0.855	0.855	0.857
6.6	0.830	0.831	0.829	0.831
6.7	0.803	0.803	0.801	0.803
6.8	0.777	0.777	0.775	0.777
6.9	0.750	0.751	0.749	0.751
7.0	0.734	0.736	0.732	0.734

Table 3. Local partial charges in electrons per unit cell.

	p band (present work)	d band (present work)	p band [2]	d band [2]
O p	6.35	1.46	6.34	1.46
Cu d	2.00	32.70	1.98	32.74
Cu s	0.22	0.35	0.24	0.33
Total	12.00	40.00	12.00	40.00

momentum region, the anisotropy values are almost zero, which depicts the long-range effect.

In figure 2 we plotted the experimental Compton profile results of Bandyopadhyay *et al* [6], the results of the LCGO calculation and the Hartree–Fock free-atom model results. The Hartree–Fock free-atom values have been calculated taking the free-atom wavefunction contribution and is an approximate model; it does not consider the interaction potential nor screening effects. Because of this it is quite evident from the figure that the $J(0)$-value is much higher than the experimentally obtained value, while in our sophisticated calculation we have considered the interaction potential which resulted in a lower $J(0)$-value close to the experimental value but is still not within the error limit at $q = 0$.

The anisotropic results are expected to provide a stringent test for the d and the p-like wavefunctions in this system. In the next section we presented the calculated DOS results based on these wavefunctions which may also be regarded as a test of validity of the basis Gaussian orbitals.

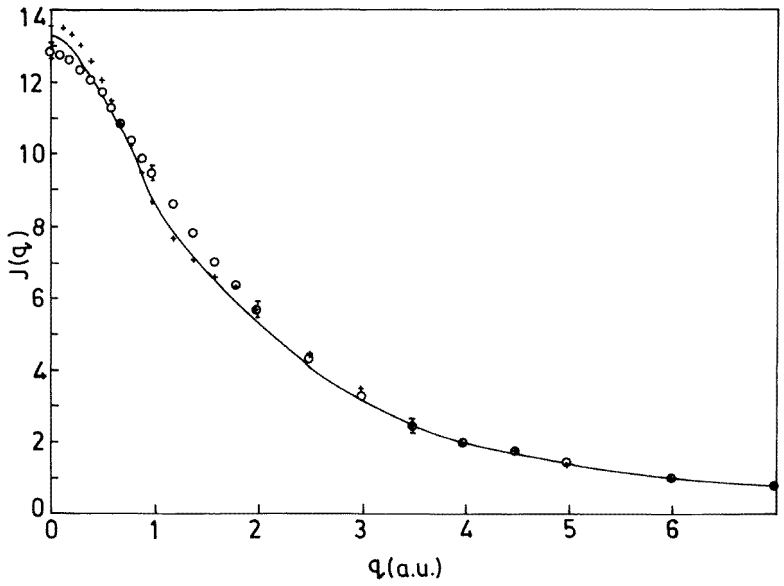

Figure 2. Total Compton profiles of Cu_2O: ——, present calculation; ○ , experimental values; +, Hartree–Fock values.

4. Density of states

The DOS was calculated by the linear tetrahedron method [33–36] using 89 points and is plotted in figure 3. There is fairly good agreement between our calculated DOS and that due to Marksteiner *et al* [2] and Ghijsen *et al* [7]. Photoelectron spectra of Cu_2O have been reported using UV [37], x-ray [38] and synchroton radiation [39]. The latter spectrum shows peaks at about 1.6, 0.44–0.51 and 0.24 Ryd below E_F, the Fermi energy. These peaks corresponds to the s, p, and d bands, respectively. In our calculation, the centres of the s and p bands lie at about 1.6 and 0.46 Ryd, respectively, below E_F. Here the low-lying band coming mainly from O 2s states is called the 's band' (which is filled with four electrons), the next band due to the oxygen 2p states (in the range between -0.45 and -0.75 Ryd) is called the 'p band' (which is filled with 12 electrons) and the band which originated from Cu 3d states (between -0.45 Ryd and E_F) is called the d band (which is filled with 40 electrons).

We thus obtained results which are in close agreement with the results reported earlier. The peak at 0.44–0.51 Ryd in the photo-emission spectrum has a very flat maximum, indicating that this structure is not fully resolved and consists of more than one peak. This observation is consistent with the double-peak structure of our p-band DOS. A more detailed comparison between photoemission spectra and DOS would require a proper calculation of transition probabilities.

After the analysis of the DOS $G(E)$, which is given by

$$G(E) = \Omega \sum_n \int \delta(E - E_{nk}) A_{nk} \, \mathrm{d}^3\boldsymbol{k} \tag{4}$$

the local partial charges are then obtained. The total DOS are given when $A_{nk} = 1$ while, the partial DOS, A_{nk} is set equal to the local partial charges as defined by Blaha and Schwarz

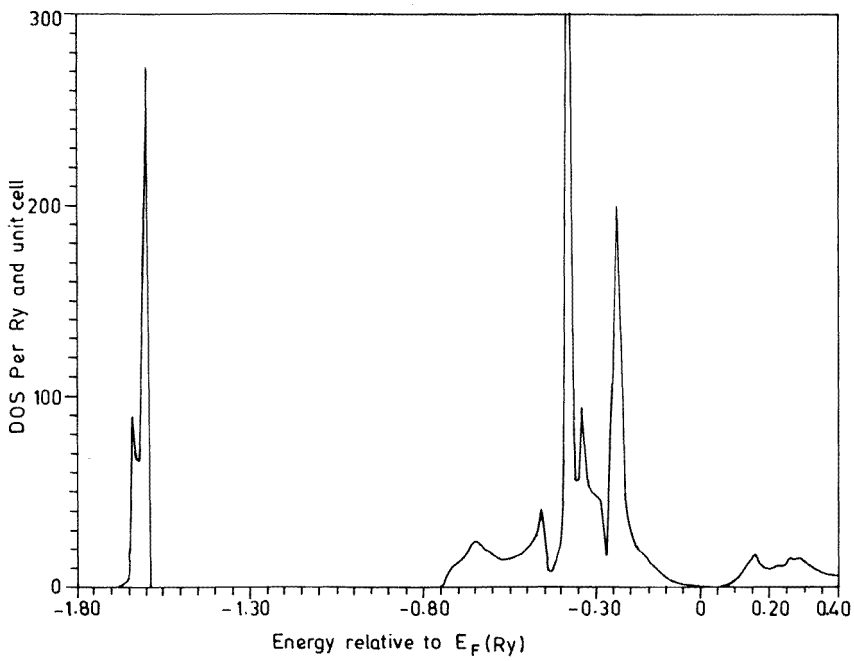

Figure 3. DOS of cuprous oxide.

et al [40]. The partial charges thus obtained are given in table 3, together with the values from previous calculations.

5. Conclusion

The Compton profile of cuprous oxide has been calculated in the present work using the LCGO method. Further the nature of the low-momentum anisotropy reflects the free-electron contribution effect. One expects cuprous oxide to show ideal ionic behaviour and to consist of Cu^+ cations with a filled d shell and O^{2-} anions. Such an ionic model to a certain extent is a good first approximation. The nature of the Cu–O bond can be interpreted from the local partial charges and the DOS. There is an extensive hybridization between the O p and Cu d states as is evident from table 3. The p-band DOS shows a two-peak structure and is dominated by the O 2p component. This kind of hybridization between the O p and Cu d states leads us to the conclusion that the O p and the Cu d components can form pdπ bonds and pdσ bonds as has been pointed out by Marksteiner *et al* [2]. It is important to mention here that the p–d interaction described above does not require an sp^3 hybrid on tetrahedrally coordinated oxygen, as is often assumed.

The Cu 4s states can hardly be seen in the DOS because of the strong decimalization of the Cu 4s charge which lies mostly outside the small copper spheres.

The loss of the Cu d electrons in the valence band is the very reason which makes an ionic model not quite adequate. An ideal Cu^+ ion would have a [d^{10}] configuration with no occupied 4s states and hence would result in a charge density which is spherically symmetric. This deviation from the ideal ionic behaviour may be called a covalent contribution rather than a polarization. The majority of the d states, however, are non-bonding, and their

covalent interaction is weak.

Furthermore another aspect which can be interpreted from the anisotropy of the charge distribution is the electric field gradient. So far the non-spherical charge density around the copper site is best described by Nagel's MSX_α-cluster calculation. With a judicious choice of all cluster parameters, he found an electric field gradient ($1.41ea_H^{-3}$) that agrees well with the value derived from the experimental quadrupole coupling constant ($1.26ea_H^{-3}$) [41]. It is important to note here that Nagel obtained a charge transfer from the copper to the oxygen atom which is much smaller than ours. This is because our band-structure calculation treats long-range order correctly and thus describes the charge-transfer effects better than a cluster model does.

For calculation of electronic structure of cuprous oxide, both the LCGO and the muffin-tin LAPW method have some shortcomings. Whereas the accuracy of the LAPW method is affected by the muffin-tin approximation, the LCGO method is affected by the choice of the Gaussian orbitals. We favour the use of an orbital basis from self-consistent field calculations [25, 26]; however, the small exponents required to describe the tails of atomic wavefunctions are not taken into consideration. It is also reasonable to delete very-long-range orbitals from the basis. This is the first report of the theoretical calculation of a Compton profile and a DOS of cuprous oxide based on the LCGO method. The importance of this work lies in the fact that we report here the directional Compton profiles of cuprous oxide. The profiles and the anisotropy are expected to provide the first stringent test for p and d-like wavefunctions in this system.

The Gaussian orbitals used in the LCGO method for the calculation of Compton profile and then the DOS and the charge analysis have been found to give hybridization of O p and Cu d which was earlier stated by Marksteiner *et al* [2]. Thus our calculation has provided further concrete proof of the results which was stated earlier by Marksteiner *et al* [2].

Acknowledgments

Dr V Sundararajan, University of Pune, helped us in this work with valuable discussions. Dr A Chatterjee of Motijheel College, Calcutta, also helped us in the analysis of the anisotropy of the Compton profile. One of the authors Shri A Deb is grateful to the Director, Bose Institute, Calcutta, for providing him with a research fellowship for continuing this work.

References

[1] See, e.g., Washington M A, Genack A Z, Cummins H Z, Bruce R H, Compaan A and Forman R A 1977 *Phys. Rev.* B **15** 2145
[2] Marksteiner P, Blaha P and Schwarz K 1986 *Z. Phys.* B **64** 119
[3] Nagel S 1985 *J. Phys. Chem. Solids* **46** 743
[4] Robertson J 1983 *Phys. Rev.* B **28** 3378
[5] Dahl J P and Switendick A C 1966 *J. Phys. Chem. Solids* **27** 931
[6] Bandyopadhyay S, Chatterjee A K, Saha S K and Chatterjee A 1994 *Radiat. Phys. Chem.* **44** 517
[7] Ghijsen J, Tjeng L H, Van Elp J, Eskes H, Westerink J, Sawatzky G A and Czyzyk M T 1988 *Phys. Rev.* B **38** 11 322
[8] Wang C S, and Callaway J 1978 *Comput. Phys. Commun.* **14** 327
[9] Callaway J and Wang C S 1977 *Phys. Rev.* B **16** 2095
[10] Wang C S, and Callaway J 1977 *Phys. Rev.* B **15** 298
[11] Laurent D G, Wang C S, and Callaway J 1978 *Phys. Rev.* B **17** 455
[12] Bagoyoko D, Zielger A and Callaway J 1983 *Phys. Rev.* B **28** 5419
[13] Laurent D G, Callaway J, Fry J L and Bremer N E 1981 *Phys. Rev.* B **23** 4877
[14] Callaway J, Zou Xianwu and Bagayoko D 1983 *Phys. Rev.* B **27** 631

[15] Laurent D J, Callaway J and Wang C S 1979 *Phys. Rev.* B **20** 1134
[16] Bagayoko D, Zielger A and Callaway J 1983 *Phys. Rev.* B **27** 7046
[17] Blaha P and Callaway J 1985 *Phys. Rev.* B **32** 7664
[18] Fuster G, Tyler J M, Brener N E, Callaway J and Bagayoko D 1990 *Phys. Rev.* B **42** 7322
[19] Jani A R, Brener N E and Callaway J 1988 *Phys. Rev.* B **38** 9425
[20] Tripathi G S, Brener N E and Callaway J 1988 *Phys. Rev.* B **38** 10 454
[21] Manninen S and Paakkari T 1991 *Phys. Rev.* B **44** 2928
[22] Jani A R, Tripathi G S, Brener N E and Callaway J 1989 *Phys. Rev.* B **40** 1593
[23] Barth von U and Hedin L 1972 *J. Phys. C: Solid State Phys.* **5** 1629
[24] Rajagopal A K, Singhal S P and Kimball J 1979 quoted by Rajagopal A K 1979 *Adv. Chem. Phys.* **41** 59
[25] Wachters A J H 1970 *J. Chem. Phys.* **52** 1033
[26] Huzinaga S 1965 *J. Chem. Phys.* **42** 1293
[27] Poirer K, Kari R and Csizmadia I G 1985 *Phys. Sci. Data.* **34**
[28] Wells A F 1984 *Structural Inorganic Chemistry* (Oxford: Claredon) p 1120
[29] Asbrink S and Norrby L J 1970 *Acta Crystallogr.* B **26** 8
[30] Williams B 1977 *Compton Scattering* (New York: McGraw-Hill) p 159
[31] Sharma B K 1993 *Z. Naturforsch.* a **48** 334
[32] Biggs F, Mendelsohn L B and Mann J B 1975 *At. Data Nucl. Data Tables* **16**
[33] Jepsen O and Anderson O K 1971 *Solid State Commun.* **9** 1763
[34] Lehman G and Taut M 1972 *Phys. Status Solidi* b **54** 469
[35] Rath J and Freeman A J 1975 *Phys. Rev.* B **11** 2109
[36] Singhal S P 1975 *Phys. Rev.* B **12** 564 6007
[37] Wertheim G K and Hiifner S 1972 *Phys. Rev. Lett.* **28** 1028
[38] Benndorf C, Caus H, Egbert B, Seidel H and Thieme F 1980 *J. Electron Spectrosc.* **19** 77
[39] Thuler M R, Benbow R L and Hurych Z 1982 *Phys. Rev.* B **26** 669
[40] Blaha P and Schwarz K 1983 *Int. J. Quant. Chem.* **23** 1535
[41] Kruger H and Mayer-Berkhout U 1952 *Z. Phys.* **132** 171